Ionic Strength Dependence of Protein Adsorption to Dye-Ligand Adsorbents

Songping Zhang and Yan Sun
Dept. of Biochemical Engineering, School of Chemical Engineering and Technology, Tianjin University, Tianjin 300072, P. R. China

The adsorption equilibria and kinetics of bovine serum albumin (BSA) and lysozyme to two Cibacron Blue 3GA (CB) modified agarose gels, that is, 6% agarose-coated steel (6AS) and Sepharose CL-6B, in 0.01 kmol·m^{-3} tris-HCl buffer (pH 7.5) were studied. Effects of aqueous-phase ionic strength on both the adsorption equilibrium and uptake rate of the proteins were significant and distinctly different between BSA and lysozyme. The adsorption of lysozyme decreased monotonically with increasing ionic strength. Ionic strengths, however, maximized BSA adsorption capacities of the two CB-modified agarose gels in the tris-HCl buffer (about 0.2 kmol·m^{-3} for CB-6AS and 0.05 kmol·m^{-3} for CB-Sepharose), when the pore-size difference of the two matrixes and electrostatic interactions between the BSA and CB molecules of like charge were considered. The effective diffusivity of BSA, derived from a pore-diffusion model, to both the CB-modified agarose gels increased significantly with the increasing ionic strength at the ionic strength range of 0.01 to 0.3 kmol·m^{-3}, due to the electrostatic interactions between the BSA and CB molecules of like charge. In contrast, the effective diffusivities of lysozyme to CB-Sepharose in the buffer containing 0.1 and 0.3 kmol·m^{-3} NaCl were nearly the same.

Introduction

Dye–ligand affinity chromatography has been widely utilized for protein purification (Arica et al., 1998; Gianazza and Arnaud, 1982; McCreath et al., 1995). Fundamental data of protein adsorption to dye–ligand affinity adsorbents, that is, adsorption equilibria and kinetics, are of great importance for the design and optimization of the purification process. It has been well known that aqueous phase ionic strength strongly affects the adsorption equilibrium of proteins to Cibacron Blue 3GA (CB) modified agarose gel, leading to the decrease of protein adsorption (Boyer and Hsu, 1990; He et al., 1997). However, little work has been reported on the effect of ionic strength on the kinetics of protein adsorption to dye–ligand adsorbents.

There is considerable experimental information on the diffusion coefficient of proteins and other macromolecules through uncharged agarose gel. It has been reported that the diffusivity of the macromolecules within a neutral agarose gel was significantly hindered and decreased with increasing protein size (Boyer and Hsu, 1992; Moussaoui et al., 1992). Studies on the diffusion of globular proteins (serum albumin, ovalbumin, and lactalbumin) through SP-Sepharose (6% sulfated agarose gel) of like charge revealed that the transport rate of the proteins depended strongly on ionic strength (Johnson et al., 1995). The effective diffusivity (D_e) was expressed by

$$D_e = \Phi D_p, \tag{1}$$

where Φ is the equilibrium partition coefficient of the negatively charged proteins between the solid phase and bulk solution, and D_p is the diffusivity within the gel phase. They showed that Φ increased significantly with increasing ionic strength, while D_p was only slightly affected by ionic strength. The increase of Φ with increasing ionic strength was considered due to the increased shielding of the repulsive electrostatic interactions (Johnson et al., 1995). The charge effects on the effective diffusivity of charged potassium polystyrene sulfonate (M_r $1.6\times10^4 - 4.1\times10^4$) in track-etch polycarbonate porous membranes of like charge showed similar results to those of Johnson et al. (1995) (Lin and Deen, 1992), and

Correspondence concerning this article should be addressed to Y. Sun.

have also been explained by theoretical predictions of the effects of ionic strength on partition coefficient. In contrast, the effective diffusivity of protein into uncharged polymers exhibited no significant dependence on ionic strength (Lin and Deen, 1992).

Because several of the aromatic rings in the CB molecule are substituted with negatively charged sulfonate groups, the dye can function as a cation exchanger to bind proteins by electrostatic interactions (Scopes, 1987). There would be electrostatic repulsion or attraction when the pH value is beyond from the isoelectric points of proteins. Therefore, ionic strength might affect not only the adsorption equilibrium but also the adsorption kinetics by influencing the electrostatic interactions between the charged proteins and CB-modified agarose gel. Furthermore, the effect of ionic strength on the adsorption of proteins with like charge and opposite charge to CB-adsorbents may also be different. Thus, in this research an acidic protein bovine serum albumin (BSA) and a basic protein lysozyme were chosen as model proteins to evaluate the effect of ionic strength on both the adsorption equilibria and kinetics to CB-modified agarose gel. Two kinds of agarose gels with different porosities were used as the base matrices. The uptake rate of the proteins was analyzed using a pore-diffusion model, and the dependence of the effective pore diffusivity of the proteins to the adsorbents on ionic strength was discussed.

Materials and Methods

Materials

Sepharose CL-6B was purchased from Amersham Pharmacia Biotech (Uppsala, Sweden). Agarose (6% cross-linked) coated steel beads ($76 \sim 152\,\mu$m) was obtained from UpFront Chromatography A/S (Copenhagen, Denmark). BSA, chicken egg white lysozyme, and Cibacron Blue 3GA (CB) were purchased from Sigma Chemical Company (St. Louis, MO). All other reagents were of analytical grade.

Adsorption equilibrium experiments

CB was covalently coupled to 6% agarose-coated steel beads (6AS) and Sepharose CL-6B, as described elsewhere (He et al., 1997). In this work, the CB coupling densities for 6AS and Sepharose CL-6B were 14.2 and 16.2 $\text{mol}\cdot\text{m}^{-3}$, respectively. These dye–ligand adsorbents were denoted as CB-6AS and CB-Sepharose, respectively.

The experiments of BSA and lysozyme adsorption to the dye–ligand adsorbents were performed in 0.01 $\text{kmol}\cdot\text{m}^{-3}$ tris-HCl buffer, pH7.5. The adsorption isotherms at different ionic strengths were generated by stirred-batch experiments as reported by Chase (1984). Generally, about 0.1 cm^3 drained gel, previously equilibrated for 24 h in the tris-HCl buffer with a definite NaCl concentration, was introduced to 10 cm^3 protein solution of known concentration. The suspension was allowed to equilibrate at 298 K on a shaking incubator at 170 rpm. After 20-h incubation, protein concentration in the supernatant was determined with a model 752C UV/VIS spectrophotometer (Shanghai Analytical Instrument Co., Shanghai, China) at 280 nm, and the adsorbed density of protein was calculated by mass balance.

Adsorption kinetics

The kinetic experiments of BSA and lysozyme adsorption to CB-Sepharose at different NaCl concentrations were performed in a stirred-batch system (He et al., 1998). Typically, 2 cm^3 of the drained gel was equilibrated in 10 cm^3 of the tris-HCl buffer with a definite NaCl concentration, and then mixed with 90 cm^3 protein solution in the same buffer with the same NaCl concentration. The suspension in a flask was mechanically agitated and the temperature was kept at 298 K with a water bath. Every few minutes, about 3 cm^3 of the liquid was pumped out of the flask through a 1-μm stainless filter to determine the protein concentration. Thereafter, the sample was returned to the vessel immediately. This procedure took less than 0.5 min. The initial concentration of BSA and lysozyme were 1.0 and 0.5 $\text{kg}\cdot\text{m}^{-3}$, respectively.

Because of the high density of the 6AS matrix (see Table 1), good mixing could not be readily realized by the agitation mentioned earlier in the kinetic experiments for protein adsorption to CB-Sepharose. Instead, the experiments of BSA uptake to CB-6AS were conducted in a shaking incubator. That is, an exactly equal mass of drained CB-6AS was added separately to a series of 10-cm^3 centrifuge tubes, all containing 5 cm^3 of 1.0 $\text{kg}\cdot\text{m}^{-3}$ BSA solution. These capped tubes containing liquid–solid suspensions were horizontally placed and shaken end to end at 298 K on a shaking incubator at 170 rpm. It was found that a good liquid and solid mixture could be reached by this shaking method. The centrifuge tubes were taken out at different time intervals to measure the supernatant protein concentrations spectrophotometrically at 280 nm. Using this procedure, the time course of the liquid-phase BSA concentration decrease was determined.

Determining the porosity of 6AS beads

Because protein adsorption to unsubstituted agarose matrices is negligible (Boyer and Hsu, 1992) and the CB dye molecule is so small that it does not alter the pore size (Horstmann et al., 1986), the effective intraparticle porosity

Table 1. Physical Properties of CB-6AS and CB-Sepharose

Adsorbent	d_p (μm)	d_i (μm)	ρ_p ($\text{kg}\cdot\text{m}^{-3}$)	f	CB density. ($\text{mol}\cdot\text{m}^{-3}$)	$\epsilon_{p,e}$(BSA)	$\epsilon_{p,e}$(Lys)
CB-6AS	138.1*	71.2*	2,980†	0.86	14.2	0.17 ± 0.01	—
CB-Sepharose	93**	—	1,040†	1	16.2	0.55††	0.75††

*Measured with a Mastersizer 2000 unit (Malvern Instruments Limited, UK).
**Data provided by the manufacturer (A. Pharmacia Biotech, Uppsala, Sweden).
†Particle density was measured using a pycnometer at 298 K.
††Data obtained from Horstmann et al. (1986).

of the CB-6AS beads for BSA can be determined using the 6AS beads with a batch-diffusion technique. The procedure is described as follows. About 3 cm^3 (V_s) of drained 6AS beads, previously equilibrated for 24 h in tris-HCl buffer (pH7.5, 0.01 $kmol \cdot m^{-3}$) was mixed with 6 cm^3 (V_L) BSA solution at 298 K on a shaking incubator for 5 h. Thereafter the liquid-phase BSA concentration was determined with a UV/VIS spectrophotometer. The apparent porosity of the beads for BSA is then estimated by

$$\epsilon_{p,a} = \frac{(c_0 - c_f)V_L}{V_s c_f}. \tag{2}$$

Triplicate experiments were carried out at initial BSA concentrations of 0.5, 1.0, and 1.5 $kg \cdot m^{-3}$, and the porosity values thus obtained were averaged and the standard deviation was determined.

The 6AS matrix is a dense pellicular composite matrix prepared by entrapping the steel sphere with agarose gel. The observation by microscopy showed that there was a single steel sphere at the center of the particle for most of the beads (picture not shown). After digesting the agarose gel around the 6AS beads with 0.5 $kmol \cdot m^{-3}$ HCl at 358 K, the inner steel sphere diameter, d_i, was determined with a Mastersizer 2000 unit (Malvern Instruments Limited, UK). Then, the average agarose gel volume fraction was calculated from

$$\left(\frac{d_i}{d_p}\right)^3 = 1 - f, \tag{3}$$

and the true effective porosity of the agarose gel in the 6AS beads for BSA was given by

$$\epsilon_{p,e} = \frac{\epsilon_{p,a}}{f}. \tag{4}$$

Kinetic Model

It is well known that there are at least three discrete steps involved in the protein adsorption from a bulk solution into a solid adsorbent, all of which contribute resistance to protein uptake. These steps include mass transfer from bulk liquid to the outer surface of the particles (film-diffusion resistance), movement by diffusion into the pores of the adsorbent (pore-diffusion or interior-diffusion resistance), and the protein binding to the pore surface (surface-reaction resistance) (Horstmann and Chase, 1989). Adsorption kinetic studies showed that the diffusion of proteins in the agarose matrix was rate-limiting in both the ion-exchange and biospecific-protein adsorption processes when compared to adsorption reaction (Horstmann and Chase, 1989; Skidmore et al., 1990). Moreover, Champluvier and Kula (1992) reported that the adsorption of glucose-6-phosphate dehydrogenase to CB-modified micromembrane could reach saturation within 1 s. Thus, in this work the adsorption was considered infinitely fast, so the concentration of proteins in the adsorbent pore was in equilibrium with the adsorbed proteins at any radial position, and a pore-diffusion model (PDM) was employed to describe protein uptake kinetics. In this model, it is assumed that intraparticle mass transfer occurs by diffusion in liquid-filled pores with a driving force expressed in terms of the pore fluid concentration gradient (Weaver and Carta, 1996; Wright et al., 1998). The basic equation for the PDM is described as

$$\epsilon_{p,e}\frac{\partial c}{\partial t} + \frac{\partial q}{\partial t} = \frac{D_e}{r^2}\frac{\partial}{\partial r}\left(r^2\frac{\partial c}{\partial r}\right), \tag{5}$$

where D_e is the effective pore diffusivity,

$$D_e = \epsilon_{p,e} D_p. \tag{6}$$

According to the model assumption, q is in equilibrium with c. In this work, protein adsorption equilibrium can be expressed by the Langmuir isotherm (see below), that is,

$$q = \frac{q_m c}{K_d + c}. \tag{7}$$

Substituting Eq. 7 into Eq. 5 gives

$$\left[\epsilon_{p,e} + \frac{q_m K_d}{(K_d + c)^2}\right]\frac{\partial c}{\partial t} = \frac{D_e}{r^2}\frac{\partial}{\partial r}\left(r^2\frac{\partial c}{\partial r}\right). \tag{8}$$

The initial and boundary conditions of the partial differential equation are given by

$$t = 0, \qquad c = 0 \tag{9a}$$

$$r = r_i, \qquad \frac{\partial c}{\partial r} = 0 \tag{9b}$$

$$r = r_p, \qquad c = c_b. \tag{9c}$$

In Eq. 9b, $r_i = 0$ for Sepharose gel, while $r_i > 0$ for 6AS particles.

From the mass balance for protein in a batch-adsorption system, the change in the liquid-phase concentration due to solid-phase uptake can be derived as

$$-H\frac{dc_b}{dt} = \frac{d\bar{q}}{dt}. \tag{10}$$

The initial condition is as follows

$$t = 0, \quad c_b = c_{b,0} \qquad \bar{q} = 0, \tag{11}$$

where $\bar{q}$ is the protein concentration in the particle averaged over the particle volume, calculated by the following formula

$$\bar{q} = \frac{\int_{r_i}^{r_p} q r^2 dr}{\int_{r_i}^{r_p} r^2 dr} \tag{12}$$

The boundary condition expressed by Eq. 9c assumes that the external-film mass-transfer resistance is negligible com-

pared to the interior diffusion. When the film mass-transfer effect is taken into account, Eqs. 9c and 10 for the model should be replaced with Eqs. 9c′ and 10′, respectively

$$r = r_p, \quad D_e \frac{\partial c}{\partial r} = k_f \left(c_b - c \,|_{r=r_p} \right) \tag{9c′}$$

$$\frac{dc_b}{dt} = -\frac{3k_f H}{r_p} \left(c_b - c \,|_{r=r_p} \right), \tag{10′}$$

where k_f is the film mass-transfer coefficient, which can be estimated from the following correlation for protein adsorption to adsorbent particles in stirred-tank experiments (Geankopolis, 1983):

$$k_f = \frac{2D_{AB}}{d_p} + 0.31 \left(\frac{\mu}{\rho D_{AB}} \right)^{-2/3} \left(\frac{\Delta \rho \mu g}{\rho^2} \right)^{1/3}. \tag{13}$$

The diffusion coefficient of proteins in free solution, D_{AB}, is 6.9×10^{-11} $m^2 \cdot s^{-1}$ for BSA and 11.8×10^{-11} $m^2 \cdot s^{-1}$ for lysozyme (Tyn and Guesk, 1990).

Equations 8 and 10 (or Eq. 10′), together with the appropriate boundary conditions, were solved numerically by the orthogonal collocation method (Weaver and Carta, 1996) to predict the change in liquid-phase protein concentration with time, and the simulation results were fitted to the dynamic adsorption data to determine the effective pore diffusivity of proteins at different ionic strengths.

Results

Properties of agarose matrices

The properties of the agarose matrices used in this work are listed in Table 1. The effective porosities of Sepharose for BSA and lysozyme were obtained according to Horstmann et al. (1986). The effective porosity of the CB-6AS matrix for BSA was determined as 0.146 ± 0.008 by the batch technique stated earlier. Taking into account the gel volume fraction in the 6AS particles (0.86; Table 1), the effective porosity of the pellicular 6AS gel for BSA was estimated to be 0.17 ± 0.01. This value was quite smaller than that of Sepharose (0.55). The result indicates that the pellicular gel in the 6AS has smaller pore size than does Sepharose CL-6B.

Adsorption isotherms

Adsorption equilibria of BSA to CB-6AS and CB-Sepharose at extensive ionic strengths were studied, and the results are shown in Figures 1 and 2. The concentrations were determined spectrophotometrically at 280 nm, and the maximum error for the data was less than 5%. The equilibrium data were fitted to the Langmuir equation (Eq. 7) by nonlinear least-squares regression using Origin 5.0 software, and the Langmuir parameters thus obtained for BSA at different NaCl concentrations are summarized in Table 2. The confidence intervals of q_m and K_d predicted by the origin 5.0 (95% confidence level) are also provided. Clearly, the Langmuir equation fitted the experimental data with small deviation at the high confidence level. The results indicated that

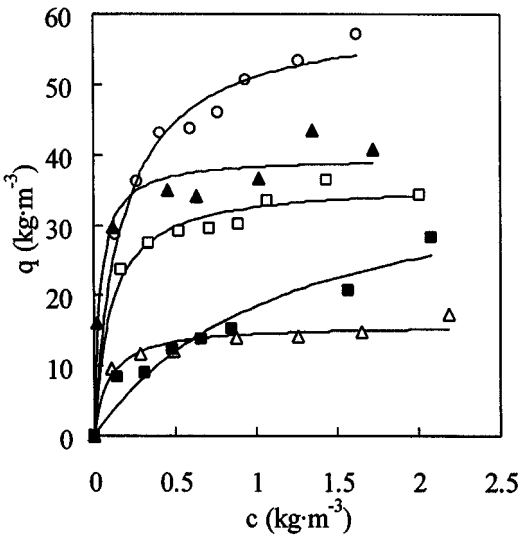

Figure 1. Adsorption isotherms of BSA to CB-6AS.

The aqueous phases are 0.01 kmol·m^{-3} tris-HCl buffer (pH 7.5) with different NaCl concentrations (kmol·m^{-3}): (△) 0.05; (□) 0.1; (○) 0.2; (▲) 0.3; (■) 0.5.

liquid-phase ionic strength affected BSA adsorption equilibria significantly, and there existed an ionic strength to give a maximal adsorption capacity of each of the dye–ligand adsorbents in the tris-HCl buffer. The adsorption capacity reached the maximum at a salt concentration of 0.2 kmol·m^{-3} for CB-6AS, and 0.05 kmol·m^{-3} for CB-Sepharose. This can be explained by considering the electrostatic interactions between the CB and BSA molecules as follows.

The CB molecule has a special chemical structure as a protein ligand, which enables it to bind to a variety of proteins

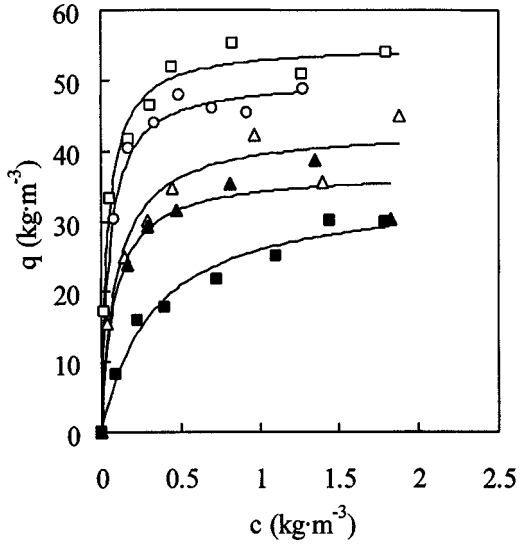

Figure 2. Adsorption isotherms of BSA to CB-Sepharose.

The aqueous phases are 0.01 kmol·m^{-3} tris-HCl buffer (pH 7.5) with different NaCl concentrations (kmol·m^{-3}): (△) 0; (□) 0.05; (○) 0.1; (▲) 0.2; (■) 0.3.

Table 2. Parameters of BSA Adsorption Equilibria and Kinetics*

Adsorbent	NaCl ($kmol \cdot m^{-3}$)	q_m ($kg \cdot m^{-3}$)	K_d ($kg \cdot m^{-3}$)	D_e^{**} (10^{-12} $m^2 \cdot s^{-1}$)	$D_e'^{\dagger}$ ($10^{-12} m^2 \cdot s^{-1}$)	Bi
CB-6AS	0.05	14.8 ± 0.7	0.118 ± 0.030	0.42	0.41	1279
	0.1	34.8 ± 1.2	0.128 ± 0.022	0.53	0.54	971
	0.2	57.0 ± 2.0	0.196 ± 0.026	1.50	1.52	345
	0.3	41.0 ± 1.5	0.036 ± 0.010	2.20	2.20	238
	0.5	38.3 ± 3.6	1.14 ± 0.34	2.00	1.90	275
CB-Sepharose	0	43.1 ± 2.3	0.095 ± 0.026	0.14	0.143	1557
	0.05	55.5 ± 1.3	0.043 ± 0.006	1.15	1.13	197
	0.1	49.1 ± 1.0	0.057 ± 0.007	2.10	2.09	106
	0.2	36.9 ± 2.4	0.080 ± 0.030	—	—	—
	0.3	34.7 ± 2.1	0.261 ± 0.070	2.90	2.86	78

*The k_f values for BSA calculated from Eq. 13 are 1.57×10^{-5} $m^2 \cdot s^{-1}$ for CB-6AS and 4.79×10^{-6} $m^2 \cdot s^{-1}$ for CB-Sepharose.
**D_e was predicted from the PDM without considering the external film mass-transfer resistance.
†D_e' was predicted from the PDM incorporating with the external film mass-transfer resistance.

according to different mechanisms such as hydrophobic interactions, affinity recognitions, and cation exchange interactions because several of the aromatic rings in the CB are substituted with negatively charged sulfonate groups (Scopes, 1987). When a CB-modified agarose adsorbent is equilibrated in tris-HCl buffer containing low-concentration NaCl, the distribution of Na^+ and Cl^- ions between the solid phase and bulk aqueous phase (that is, between the pore wall and the solution filled in the pore) can result in an accumulation of positive charge in the solution and negative charge in the adsorbent phase. This creates a difference in the electrostatic potential between the two phases, that is, the Donnan potential (Ståhlberg, 1999). Because BSA, with an isoelectric point (pI) of 4.9 (Lehninger, 1982), also carries a net negative charge at pH 7.5, there exists electrostatic repulsion between the negatively charged BSA and CB molecules. With the increase in ionic strength, the solid surface charges become more shielded by the counterions in the solution, resulting in a decrease in electrostatic potential and the repulsive force, which leads to the enhancement of BSA adsorption. On the other hand, increasing ionic strength could result in the intense binding of dye–ligand to the agarose matrix (Liu et al., 1984; Liu and Stellwagen, 1987), leading to the decrease in the ligand density accessible to protein, which was unfavorable for protein adsorption. These two opposite effects of ionic strength on BSA adsorption would result in the presence of an ionic strength that maximizes BSA adsorption. Furthermore, with the complex effect of ionic strength, the Langmuir dissociation constant showed a nonmonotonic trend with ionic strength. As discussed earlier, the 6AS gel has a smaller pore size than Sepharose CL-6B. At a very low ionic strength, the Donnan exclusion could greatly shield the pores in the CB-6AS gel, resulting in a high exclusion of BSA molecules from entering the gel, and a low BSA adsorption capacity (Figure 1). In the extreme case, little BSA adsorption was observed when no NaCl was included in aqueous phase (data not shown). For CB-Sepharose, however, a high, albeit not maximum, BSA adsorption was observed, even though NaCl was absent. This is due to the contribution of the larger pores in this agarose gel.

Lysozyme adsorption equilibria to CB-Sepharose at different ionic strengths were also studied. The isotherms are illustrated in Figure 3, and the values of q_m and K_d obtained by fitting Eq. 7 to the experimental data are listed in Table 3. Lysozyme, with a pI of 11.2 (Lehninger, 1982), is positively charged at pH 7.5 and could bind to the dye–ligand adsorbent by strong electrostatic interactions. Hence, at very low ionic strength (0.01 $kmol \cdot m^{-3}$ tris-HCl buffer), its adsorption isotherm was nearly rectangular, that is, the adsorption was almost irreversible. Lysozyme adsorption capacity decreased significantly with increasing ionic strength, both due to the decrease in electrostatic interactions and the decrease in the accessible ligand density by binding to the matrix (Liu et al., 1984; Liu and Stellwagen, 1987). This is a typical phenomenon encountered in lysozyme adsorption to CB-modified agarose gel (Boyer and Hsu, 1990).

Adsorption kinetics

The uptake curves of BSA and lysozyme to CB-6AS and/or CB-Sepharose at different ionic strengths are exhibited in Figures 4 to 6. The solid lines in the figures were calculated from the PDM with or without considering the effect of film

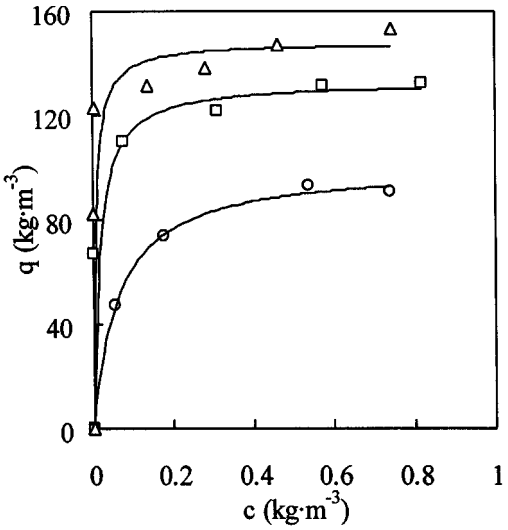

Figure 3. Adsorption isotherms of lysozyme to CB-Sepharose.

The aqueous phases are 0.01 $kmol \cdot m^{-3}$ tris-HCl buffer (pH 7.5) with different NaCl concentrations ($kmol \cdot m^{-3}$): (△) 0; (□) 0.1; (○) 0.3.

Table 3. Parameters of Lysozyme Adsorption Equilibria and Kinetics to CB-Sepharose*

NaCl (kmol·m^{-3})	q_m (kg·m^{-3})	K_d (kg·m^{-3})	D_e** (10^{-11} m^2·s^{-1})	D_e'† (10^{-11}m^2·s^{-1})	Bi
0	148.6±0.5	0.007±0.003	1.9	2.5	15.2
0.1	132.8±5.2	0.054±0.021	3.3	4.8	7.9
0.3	104.5±2.1	0.082±0.006	3.2	4.5	8.4

*The k_f value for lysozyme calculated from Eq. 13 was 8.18×10^{-6} m·s^{-1}.
**D_e was predicted from the PDM without considering the external film mass-transfer resistance.
†D_e' was predicted from the PDM incorporating with the external film mass-transfer resistance.

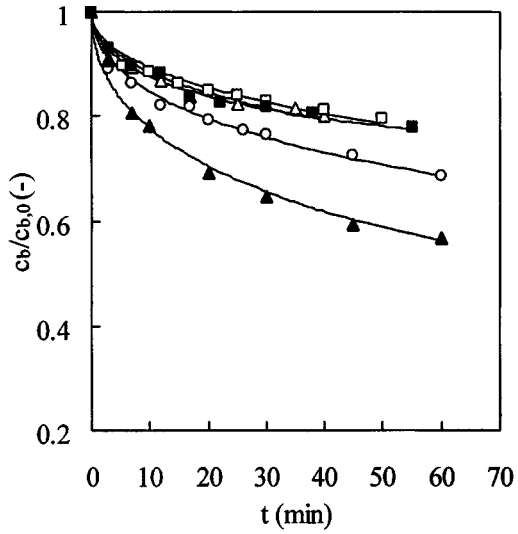

Figure 4. Dynamic uptake profiles of BSA by CB-6AS.

The aqueous phases are 0.01 kmol·m^{-3} tris-HCl buffer (pH 7.5) with different NaCl concentrations (kmol·m^{-3}): (△) 0.05; (□) 0.1; (○) 0.2; (▲) 0.3; (■) 0.5. The solid lines are calculated from the PDM.

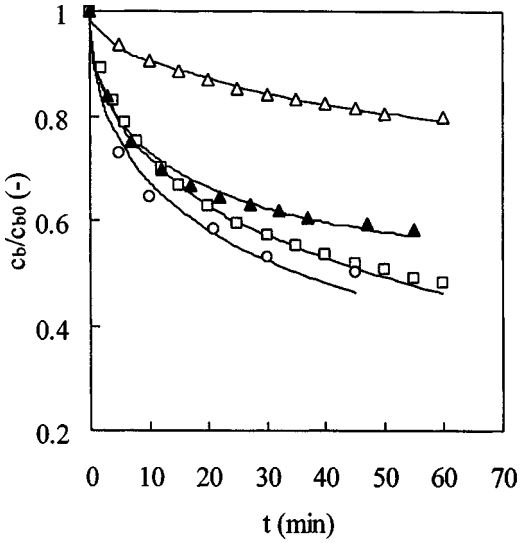

Figure 5. Dynamic uptake profiles of BSA by CB-Sepharose.

The aqueous phases are 0.01 kmol·m^{-3} tris-HCl buffer (pH 7.5) with different NaCl concentrations (kmol·m^{-3}): (△) 0; (□) 0.05; (○) 0.1; (▲) 0.3. The solid lines are calculated from the PDM.

mass-transfer resistance. It can be seen that the PDM predicts the adsorption kinetics well. The values of the effective pore diffusivity for BSA and lysozyme thus obtained are listed in Tables 2 and 3, respectively. At the same time, the values of the effective pore diffusivity (De') predicted by the PDM incorporating with the external film mass-transfer resistance are also listed in Tables 2 and 3.

Table 2 indicates that for BSA adsorption to both the adsorbents, the effective pore diffusivities predicted from the PDM with and without considering the external film mass-transfer resistances are nearly the same. For lysozyme adsorption, however, relatively large difference between D_e and De' can be observed (Table 3). That is, for BSA adsorption the effect of film mass resistance can be neglected, while for lysozyme it cannot be neglected compared to the interior diffusion. The Biot number (Eq. 14), typically used to assess the significance of film mass transfer versus intraparticle mass-transfer resistances (Do et al., 1990), was calculated and the results are provided in Tables 2 and 3

$$Bi = \frac{k_f(r_p - r_i)}{D_e}. \tag{14}$$

The Bi values for BSA adsorption were larger than 77, so

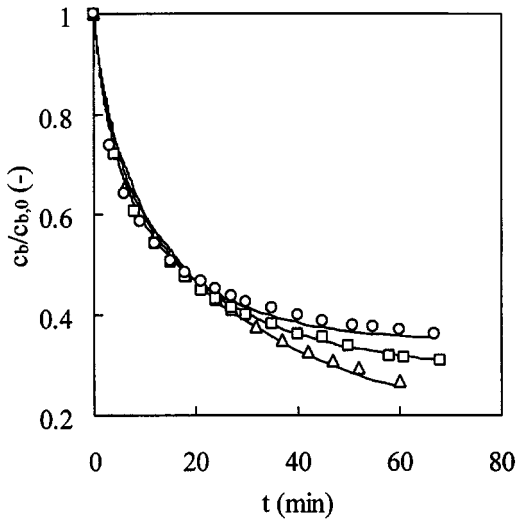

Figure 6. Dynamic uptake profiles of lysozyme by CB-Sepharose.

The aqueous phases are 0.01 kmol·m^{-3} tris-HCl buffer (pH 7.5) with different NaCl concentrations (kmol·m^{-3}): (△) 0; (□) 0.1; (○) 0.2. The solid lines are calculated from the PDM.

neglecting the external film mass-transfer resistance was reasonable to simplify the PDM model. For lysozyme, however, the *Bi* values were smaller than 16, so the external film resistance could not be neglected (Wright et al., 1998; Weaver and Carta, 1996).

Discussion

The results listed in both Tables 2 and 3 suggested that ionic strength significantly affected not only the adsorption equilibrium but also the adsorption kinetics. In addition, the relationship between adsorption and ionic strength for different proteins was of distinct difference. This is discussed in the following sections.

BSA uptake by CB-6AS and CB-Sepharose

There are several publications on the dependence of the probe diffusion of submicron-sized particles such as polystyrene spheres in aqueous solutions of polyelectrolytes on ionic strength (Phillies, et al., 1987, 1989). It has been reported that the diffusion coefficient always increases with increasing ionic strength until reaching a plateau at a high ionic strength. However, little data are available for the effect of ionic strength on protein diffusion into adsorbents under favorably adsorptive conditions.

Regarding BSA diffusion to the dye–ligand adsorbents that we are concerned with, as illustrated in Table 2, the D_e value of BSA decreases with the decrease in aqueous phase ionic strength. As mentioned earlier, there exists electrostatic repulsion between the BSA and CB molecules, and it would increase with decreasing ionic strength. Therefore, the electrostatic repulsion between the overall negatively charged protein surface and the negatively charged pore surface can exclude proteins from the gel matrix. The electrostatic exclusion would enhance the size exclusion of BSA from the gel matrix, intensifying the hindrance of BSA transport, thus decreasing its adsorption capacity and effective pore diffusivity by decreasing ionic strength.

According to electrostatic theory, there are diffuse electrical double layers surrounding the charged protein and near to the pore surface of the CB-modified agarose gel. It can be calculated that the Debye length, κ^{-1}, the characteristic length for electrostatic interactions in electrolyte solutions, ranges from 3 nm at 0.01 kmol·m^{-3} ionic strength to 0.3 nm at 1.0 kmol·m^{-3}. Considering the electrostatic repulsion effect, we define an *effective* pore diameter of the gel matrix as follows

$$d_e = d - 2\kappa^{-1} \qquad (I \geq 0.01\,\text{kmol}\cdot m^{-3}), \qquad (15)$$

where d is the pore diameter of gel matrix, and d_e is the *effective* pore diameter for protein to diffuse in. Bosma and Wesselingh (1998) claimed that the average pore diameter of Sepharose CL-6B was about 35 nm, while Johnson et al. (1995) calculated that the average distance between agarose fibers in 6% agarose gel was 11 nm. Furthermore, agarose gel, a kind of cross-linked rigid polysaccharide, does not swell or shrink when exposed to changes in ionic strength (Johnson et al., 1995; Boyer and Hsu, 1990). That is, the true porosity and pore diameter should be physically constant with the change of ionic strength. Thus, at lower ionic strength the electrical double layers would account for a significant fraction of the interfiber spacing. Taking into account the molecular dimensions of BSA, $4\times4\times14$ nm (Bosma and Wesselingh, 1998), the protein molecules located at almost any sterically allowed positions in the CB-modified gel should experience the electrostatic exclusion effect. By increasing ionic strength, the electric double layer can be compressed, and the *effective* pore diameter for BSA increases, thus facilitating the hindered pore diffusion. At high ionic strength, the small ratio of the Debye length to interfiber spacing resulted in minimized electrostatic exclusion effect, therefore a plateau of the D_e was predicted at ionic strength higher than 0.3 kmol·m^{-3} (see Table 2).

In the PDM, the effective porosity of the gels for BSA was taken as a constant. However, research on the diffusion of globular proteins (that is, BSA, ovalbumin and lactalbumin) through SP-Sepharose carrying a like charge with the proteins indicated that the partition coefficient Φ of proteins increased more than twice when the ionic strength increased from 0.01 kmol·m^{-3} to 1.01 kmol·m^{-3}. This trend was explained by taking into account the electrostatic interactions between protein and SP-Sepharose of like charge. There have been attempts to theoretically predict the effect of the electrostatic effects on the partitioning (Johnson and Deen, 1996; Lin and Deen, 1992). Under nonadsorbing conditions, the partition coefficient Φ is equal to the effective porosity of particles for a specific protein. Accordingly, with the increase of ionic strength, the enhancement in *effective* pore diameter of agarose gel could lead to the increase in the effective porosity for BSA within the CB-modified agarose gel, resulting in the increase in the effective pore diffusivity. That is, the increase in the effective pore diffusivity with increasing ionic strength might also be partly ascribed to the increase in the effective porosity (see Eq. 6). Therefore, both the increase in the effective porosity and the decrease in the electrostatic repulsion with increasing ionic strength resulted in the increase in the D_e value of BSA to CB-modified agarose gels.

Johnson et al. (1995) reported that the D_e value of BSA into SP-Sepharose of like charge increased about twice when the ionic strength increased from 0.01 kmol·m^{-3} to 1.01 kmol·m^{-3}. In this work, the increase in the D_e value with increasing ionic strength was more than five times for CB-6AS and about 20 times for CB-Sepharose in narrower ionic strength ranges (Table 2). The results indicate that the effect of ionic-strength on the effective pore diffusivity of BSA into adsorbents of like charge under adsorbing conditions is more significant than on that into a matrix with no protein adsorption.

Lysozyme uptake by CB-Sepharose

As stated earlier, lysozyme is positively charged at pH 7.5, and its adsorption capacity decreased significantly with increasing ionic strength because of the decrease in electrostatic interactions and the decrease in the accessible ligand density by binding to the matrix. Thus, the relationship between the effective pore diffusion coefficient and ionic strength was also different from that of BSA. As indicated in Table 3, the D_e values of lysozyme in 0.01 kmol·m^{-3} tris-HCl

buffer containing 0.1 and 0.3 kmol·m^{-3} NaCl were nearly the same. When no NaCl was included, however, the D_e value was about 40% smaller. This might be due to the very strong binding of lysozyme at a very low ionic strength. That is, the adsorption was nearly irreversible, so little surface diffusion was present under this condition. At higher ionic strength, the adsorption isotherms had larger dissociation constants (Table 3), and surface diffusion could contribute somewhat to the overall mass-transport rate described by the effective pore diffusivity. The same thing can be said for the interior BSA diffusion. That is, the D_e values for BSA and lysozyme predicted from the PDM was a parameter characterizing the parallel contributions of pore diffusion and surface diffusion when the adsorption was beyond an irreversible isotherm (Miyabe and Guiochon, 2000; Yoshida et al., 1994).

Conclusions

It was shown that ionic strength has a significant effect on both protein adsorption equilibria and kinetics to two kinds of CB-modified agarose gels by affecting the electrostatic interactions between charged proteins and the dye–ligand adsorbents. Because the electrostatic interactions can be repulsive or attractive due to the difference in the isoelectric points of proteins, the effect of ionic strength on the adsorption of BSA and lysozyme is distinctly different. There exist ionic strengths that maximize the adsorption capacities of BSA to both the dye–ligand adsorbents, while the effective diffusivity of BSA into the gels increased when the ionic strength increased. The results were explained by considering the electrostatic repulsion between the negatively charged BSA and CB molecules. Increasing ionic strength can decrease the BSA exclusion that results from the electrostatic repulsion, leading to an increase in adsorption capacity and effective porosity (*effective* pore diameter), thus facilitating the hindered pore diffusion. These effects result in an increase in the effective pore diffusivity when ionic strength increases below 0.3 kmol·m^{-3}. In contrast, for the positively charged lysozyme, its adsorption decreases monotonically with increasing aqueous-phase ionic strength and the effective pore diffusivities of lysozyme to CB-Sepharose in the buffer containing 0.1 and 0.3 kmol·m^{-3} NaCl were nearly the same.

Acknowledgment

This work was supported by the National Natural Science Foundation of China (grant No. 20025617).

Notation

Bi = Biot number, $= k_f(r_p - r_i)/D_e$
c = protein concentration in pore, kg·m^{-3}
c_b = bulk-phase protein concentration, kg·m^{-3}
c_0 = initial BSA concentration in Eq. 2, kg·m^{-3}
$c_{b,0}$ = initial bulk-phase protein concentration, kg·m^{-3}
c_f = final BSA concentration in Eq. 2, kg·m^{-3}
d = pore diameter of agarose gel, m
d_e = *effective* pore diameter defined by Eq. 15, m
d_i = mean diameter of the steel sphere inside the 6AS matrix, m
d_p = mean particle diameter, m
D_{AB} = molecular diffusivity of protein in free solution, m^2·s^{-1}
D_e = effective pore diffusivity, m^2·s^{-1}
D_e' = effective pore diffusivity predicted by the PDM incorporating with the external film mass transfer, m^2·s^{-1}
D_p = pore diffusivity, m^2·s^{-1}
f = average gel volume fraction
H = volume ratio of solid-to-liquid phases
I = ionic strength, kmol·m^{-3}
K_d = dissociation constant for the Langmuir isotherm, kg·m^{-3}
k_f = liquid-film mass-transfer coefficient, m·s^{-1}
q = adsorbed protein density in equilibrium with c, kg·m^{-3}
q_m = adsorption capacity for the Langmuir isotherm, kg·m^{-3}
$\bar{q}$ = particle-average protein concentration, kg·m^{-3}
r_i = mean radius of steel sphere inside the 6AS matrix, m
r_p = mean particle radius, m
t = time, s

Greek letters

$\epsilon_{p,e}$ = effective gel porosity for proteins
$\epsilon_{p,a}$ = apparent particle porosity for the 6AS matrix in Eq. 2
κ^{-1} = Debye length, m
μ = liquid viscosity, Pa·s
ρ = liquid density, kg·m^{-3}
ρ_{gel} = density of dye-ligand adsorbent, kg·m^{-3}
$\Delta\rho$ = density difference between the solid and liquid phases, kg·m^{-3}

Literature Cited

Arica, M. Y., H. N. Testereci, and A. Denizli, "Dye–ligand and Metal Chelate Poly(2-Hydroxyethylmethacrylate) Membranes for Affinity Separation of Proteins," *J. Chromatog. A*, **799**, 83 (1998).
Bosma, J. C., and J. A. Wesselingh, "pH Dependence of Ion-Exchange Equilibrium of Proteins," *AIChE J.*, **44**, 2399 (1998).
Boyer, P. M., and J. T. Hsu, "Adsorption Equilibrium of Proteins on a Dye–ligand Adsorbent," *Biotechnol. Tech.*, **4**, 61 (1990).
Boyer, P. M., and J. T. Hsu, "Experimental Studies of Restricted Protein Diffusion in an Agarose Matrix," *AIChE J.*, **38**, 259 (1992).
Champluvier, B., and M. R. Kula, "Dye-Ligand Membranes as Selective Adsorbents for Rapid Purifications of Enzymes: A Case Study," *Biotechnol. Bioeng.*, **40**, 33 (1992).
Chase, H. A., "Prediction of the Performance of Preparative Affinity Chromatography," *J. Chromatog.*, **297**, 179 (1984).
Do, D. D., and R. G. Rice, "Applicability of External Diffusion Model in Adsorption Studies," *Chem. Eng. Sci.*, **45**, 1419 (1990).
Geankopolis, C. J., *Transport Processes and Unit Operations*, 2nd ed., Allyn & Bacon, New York (1983).
Gianazza, E., and P. Arnaud, "A General Method for Fractionation of Plasma Proteins: Dye-Ligand Affinity Chromatography on Immobilized Cibacron Blue F3-GA," *Biochem. J.*, **201**, 129 (1982).
He, L.-Z., Y. R. Gan, and Y. Sun, "Adsorption-Desorption of BSA to Highly Substituted Dye-Ligand Adsorbent: Quantitative Study of the Effect of Ionic Strength," *Bioprocess Eng.*, **17**, 301 (1997).
He L.-Z., X. Y. Dong, and Y. Sun, "A Diffusion Model of Protein and Eluant for Affinity Filtration," *Biochem. Eng. J.*, **2**, 53 (1998).
Horstmann, B. J., and H. A. Chase, "Modeling the Affinity Adsorption of Immunoglobulin G to Protein A Immobilized to Agarose Matrices," *Chem. Eng. Res. Des.*, **67**, 243 (1989).
Horstmann, B. J., C. N. Kenney, and H. A. Chase, "Adsorption of Proteins on Sepharose Affinity Adsorbents of Varying Particle Size," *J. Chromatog.*, **361**, 179 (1986).
Johnson, E. M., D. A. Berk, R. K. Jain, and W. M. Deen, "Diffusion and Partitioning of Proteins in Charged Agarose Gels," *Biophys. J.*, **66**, 1561 (1995).
Johnson, E. M., and W. M. Deen, "Electrostatic Effect on the Equilibrium Partitioning of Spherical Colloids in Random Fibrous Media," *J. Colloid Interface Sci.*, **178**, 749 (1996).
Lehninger, A. L., *Principles of Biochemistry*, Worth Publishers, New York (1982).
Lin, N. P., and W. M. Deen, "Charge Effects on Diffusion of Polystyrene Sulfonate Through Porous Membranes," *J. Collid Interface Sci.*, **153**, 483 (1992).
Liu, Y. C., R. Ledger, and E. Stellwagen, "Quantitative Analysis of Protein: Immobilized Dye Interaction," *J. Biol. Chem.*, **259**, 3796 (1984).
Liu, Y. C., and E. Stellwagen, "Accessibility and Multivalency of Immobilized Cibacron Blue F3GA," *J. Biol. Chem.*, **262**, 583 (1987).

McCreath, G. E., H. A. Chase, R. O. Owen, and C. R. Lowe, "Expanded Bed Affinity Chromatography of Dehydrogenases from Bakers' Yeast Using Dye-Ligand Perfluoropolymer Supports," *Biotechnol. Bioeng.*, **48**, 341 (1995).
Miyabe, K., and G. Guiochon, "Kinetic Study of the Mass Transfer of Bovine Serum Albumin in Anion-Exchange Chromatography," *J. Chromatog.*, **866**, 147 (2000).
Moussaoui, M., M. Benlyas, and P. Wahl, "Diffusion of Proteins in Sepharose Cl-B gels," *J. Chromatog.*, **591**, 115 (1992).
Phillies, G. D. J., C. Malone, K. Ullmann, G. S. Ullmann, J. Rollings, and L. P. Yu, "Probe Diffusion in Solution of Long-Chain Polyelectrolytes," *Macromol.*, **20**, 2280 (1987).
Phillies, G. D. J., T. Pirnat, M. Kiss, N. Teasdale, D. Maclung, H. Inglefield, C. Malone, A. Rau, L. P. Yu, and J. Rollings, "Probe Diffusion in Solutions of Low Molecular Weight Polyelectrolytes," *Macromol.*, **22**, 4068 (1989).
Scopes, R. K., "Dye-Ligands and Multifunctional Adsorbents: An Empirical Approach to Affinity Chromatography," *Anal. Biochem.*, **165**, 235 (1987).
Skidmore, G. L., B. J. Horstmann, and H. A. Chase, "Modeling Single-Component Protein Adsorption to the Cation Exchanger S-Sepharose FF," *J. Chromatog.*, **498**, 113 (1990).
Ståhlberg, J., "Review: Retention Models for Ions in Chromatography," *J. Chromatog.*, **855**, 3 (1999).
Tyn, M. T., and T. W. Guesk, "Prediction of Diffusion Coefficients of Proteins," *Biotechnol. Bioeng.*, **35**, 327 (1990).
Weaver, L. E., and G. Carta, "Protein Adsorption on Cation Exchangers: Comparison of Macroporous and Gel-Composite Media," *Biotechnol. Prog.*, **12**, 342 (1996).
Wright, P. R., F. J. Muzzio, and B. J. Glasser, "Batch Uptake of Lysozyme: Effect of Solution Viscosity and Mass Transfer on Adsorption," *Biotechnol. Prog.*, **14**, 913 (1998).
Yoshida, H., M. Yoshikawa, and T. Kataoka, "Parallel Transport of BSA by Surface and Pore Diffusion in Strongly Basic Chitosan," *AIChE J.*, **40**, 2034 (1994).

Manuscript received Jan. 23, 2001, and revision received June 6, 2001.